Snow Cover Assessment and Delineation of Hunza River Basin Using Snow Tool & ArcGIS and Correlating with Climatic Normals. (2003 to 2011)

By:

Basit Ali Qazi (04111613014)

Supervisor:

Dr. Anees Bangash

Department of Earth Sciences, (QAU)

Co-Supervisor:

Mr. Adnan Shafeeq Rana

Department of RMT, (PMD)

Department of Earth Sciences

Faculty of Geo-Physics

Quaid-I-Azam University Islamabad

2016-2020

CERTIFICATE

It is certified that **Mr. Basit Ali Qazi (Registration No. 04111613014)** carried out the work contained in this dissertation under my supervision and accepted in its present form by Department of Earth Sciences as satisfying the requirements for the award of **BS Degree in Geophysics.**

RECOMMENDED BY

Dr. Anees Ahmad Bangash
Assistant Professor/Supervisor _____

External Examiner _____

Dr. Aamir Ali
Chairman _____

DEPARTMENT OF EARTH SCIENCES
QUAI-I-AZAM UNIVERSITY
ISLAMABAD

Acknowledgement

First and foremost, I am deeply grateful to Almighty Allah who gave me the strength to complete my work with determination and fortitude. His countless blessings and favors eased out my work and gave me the aptitude to this research with purpose and produced meaningful results.

I am especially indebted to my honorable supervisor **Prof. Dr. Anees Bangash** who acted as an inspiration from day one and his constant support and care enabled me to choose my topic of interest.

I want to acknowledge the efforts of Dr. **Farrukh Bashir (PMD)** and **Adnan Shafeeq Rana (PMD)** for the time he invested in me and opened a gate way into a world of research, and his contribution to this field of research being the forerunner in high-altitude meteorology in Pakistan. I want to thank **Mr. Haroon (PMD)** and **Mr. Ehsan (PMD)** for supervising me in software tools and datasets.

I especially acknowledge the prayers, endless love, efforts, and support for my whole family notably my father **Mr. Farooq Qazi**, my lovely fellows, especially **Danish Zia**. Without whom I was unable to reach at this stage

Basit Ali Qazi
Geo-Physics
2016-2020

Contents

Abstract

Pakistan is an arid to semi-arid country with rainfall contributing only ~10% to agriculture. Agriculture of Pakistan thus depends on irrigation system constituted by a gigantic chain of hydraulic structure. Pakistan is largely dependent on its frozen hydrological resources, i.e., snow cover and glaciated ice on the mountains of Northern Pakistan. In mountain areas, where snow melt runoff often makes up a large part of river discharge, the cryosphere is a key source of water. In contrast to Global warming, the Karakoram Region is having a positive mass balance after the late 20th century. Due to higher rate pf precipitation at elevation regimes, the ice cover is increasing as contrast to melting snow caps over the world. This is termed as the 'Karakoram Anomaly' (Hewitt,2005). Snow cover assessment and Hunza river basin catchment delineation was carried out in research and the results are contrary to the Karakoram Anomaly as snow cover is decreasing from 2003-2011.Further relation was made with rainfall and temperature and it was concluded that mean temperature is of inverse to the snow cover with no relation to rainfall.

Chapter 1

General Hydrogeological and climatic setup of the study area

1 Introduction

1.1 Hindu-Kush KARAKORAM-Himalaya

Mountains and oceans play a significant role in the global climate. The Hindu Kush-Himalayas (HKH) is considered as third pole attributed to its vast spatial snow and glacial content. These mountains can have their own unique climate and the details are often misunderstood.

The Hindu-Kush Karakoram Himalaya (HKH) region is the largest mountain ranges in the world, encompassing parts of the entire countries of Bangladesh, Afghanistan, China, Bhutan, Nepal, India, Pakistan, and Myanmar. HKH region feeds some of the main rivers in Southeast Asia (such as the Ganges, the Indus the Brahmaputra, the Yang-Tze and the Yellow River,), which bring water to more than 1.5 billion people[1].

Central Mountains have elevation between 2000 and 5000 m. The Siwalik range which is made up of erosion material from the rising Himalaya which have about 1200 m elevation of. Critically important geo-ecological asset the HKH region is the origin of 10 major river basins and covers over 4.2 million km^2 area[2].

1.2 Geology of Hindu Kush-Himalaya

Pamir Mountains plateau at the border of the North-West Frontier Province of Pakistan and Afghanistan, HKH region covers over some 3,500 km to its south eastern borderline in Bhutan, Bangladesh, and Myanmar. Southward the Indo Gangetic plains border on the Hindu Kush-Himalaya region, extend from the Indus valley in Pakistan to the Brahmaputra valley in India (Assam) and the lowlands of Bangladesh. In the north the mountain ranges is bordered by the high Plateau of Tibet[3].

The Himalaya region comprises of recent and continuing tectonic uplift which began less than 130 million years ago. Great areas of metamorphic rocks in the central core of the Himalayan have been dated to the Tertiary which started before 65 million years and ended 1.6 million years ago[4].

As a direct result of the great mountain building process. Crystalline, predominantly, and metamorphic rocks make up this central Himalayan zone with gneisses, granites, schists, and sediments. Nevertheless[5]. HKH ranges contain rock series from all major periods. Thus, the eastern Himalayas there are examples of Archaean (more than 2.5 billion years old) basement gneiss, the lower ranges along the southern flank comprise a composite set of younger Tertiary sedimentary deposits which includes riverine deposits by rivers emergent onto the plains from the Himalayas[6].

1.3 Upper Indus Basin

The mountain ranges surrounding the Tibetan Plateau are a complex highland-lowland hydrologic system involves a range of water supply and use environments[1]. The importance of the Mountain contribution to the total flow of the major rivers of Asia and the sources of runoff within individual mountain catchment basins varies throughout the region. Additionally, to the limited studies of the general hydrology of the mountain catchments of these rivers[7]. There are major issues of water use as populations grow inexorably and many Asian countries begin a transition from agriculture-based systems to more industrialized economies[8].

While there is a long history of scientific visits to Karakoram Himalaya, most have been primarily exploratory resulting more in description than analysis [9]. Much of the present understanding of the hydrology, climate, and glaciers of these mountains is based on a few analyses of a very limited data base. Archer et al. discussed in 2010 that the extremely limited number of climate stations in the Upper Indus Basin (UIB). In an area of over 160,000 km^2 above the Tarbela Reservoir there are only 5 hydrometric stations in the main stem of the Indus River at the present time and fewer than 20 manual climate stations [6]. More than 250 climate stations in a comparable area in the Nepal Himalaya and this compares with a total of 28 hydrometric stations. Credible recent glacier mass balance data is available for few glaciers in the Karakoram, the Biafo, (for example, Hewitt 2010) and the Baltoro, and the Chhote Shigri Glacier in the Chenab Basin in the western Himalaya [10].

1.4 Indus river

Indus River is an international river with headwater tributaries in China (Tibet), Pakistan, India, and Afghanistan. The river originates from north of the Great Himalaya on the Tibetan Plateau. The main stem of the river runs through the Ladakh district of Jammu and Kashmir and then enters the northern areas of Pakistan (Kharmang Gilgit-Baltistan) flowing between the western Himalaya

and Karakoram Mountains [11]. Along this reach of the river stream flow volume is increased by gauged tributaries entering the main river from catchments in the Karakoram Mountains. the western Himalaya, and Shyok, Shigar, Hunza, Gilgit, the Astore River as well as ungauged basins on the north slope of the western Himalaya. Immediately north of Mt. Nanga Parbat the westernmost of the high peaks of the Himalaya, the river turns in a south direction and flows along the entire length of Pakistan that merge into the Arabian Sea near the port city of Karachi that situated in Sindh province. Tributaries to this reach of the river from the western Himalaya are the Chenab, Jhelum, Sutlej Rivers, and Ravi, from the Indian states of Himachal Pradesh, and Jammu Kashmir and the Swat, Kabul, and Chitral Rivers from the Hindu Kush Mountains. Total length of the river is 1,976 miles[12].

MAP 1 Indus Catchment [12]

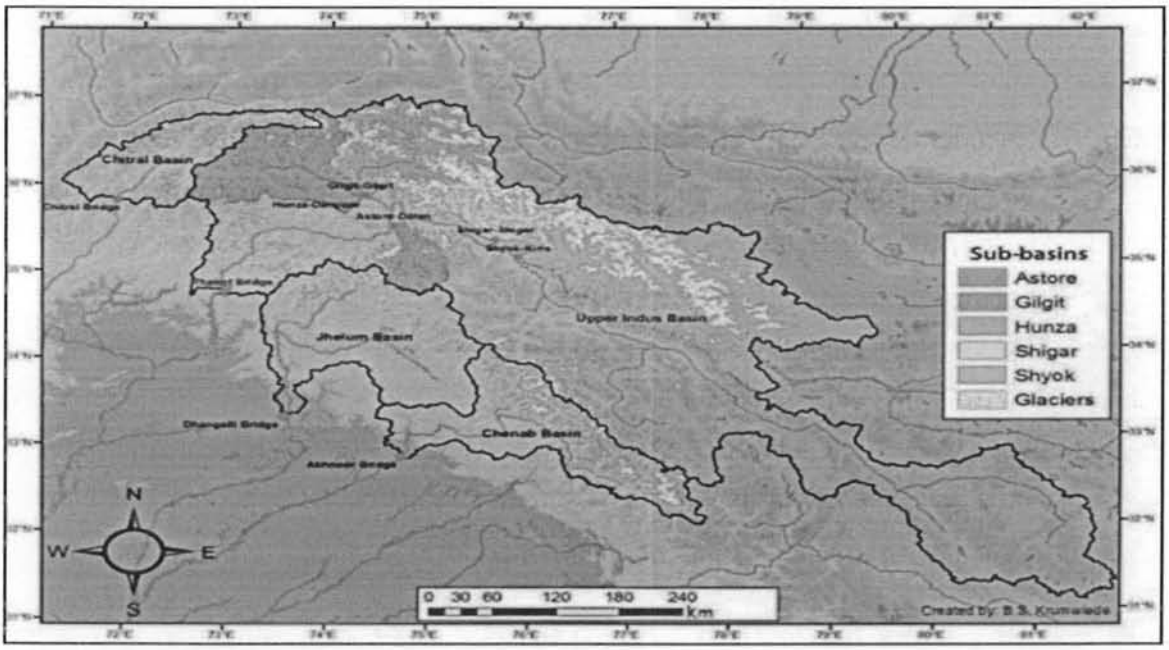

1.5 Hydrology of upper and Indus basin

General hydrology of the Lower Indus Basin is assumed to be reasonably well-understood as studied from a network of gauging stations, reservoirs such as the Mangla and Tarbela and irrigation barrages on the piedmont. While this network provides data on which management decisions concerning water uses in the lower basin can be based the hydrology of the upper basin remains a "black box" [13].

- Mean annual flow of the upper and Indus basin is about 58 MAF from the main stem above Tarbela Reservoir, Basin, 22 MAF from the Chenab Basin, 6 MAF from the Chitral Basin, and 24 MAF from the Jhelum, for a total of 110 MAF[14].
- The Total area of the Indus above Tarbela is around 166,000 km^2 with an estimated glacier area of approximately 17,000 km^2. The other glacierized the Chenab in the western Himalaya has a surface area of 22,500 km^2 and glacier area of 2,700 km^2 [15].
- Two principal sources of runoff from the upper and Indus basin are.

  (1) Winter precipitation, snow that melts in the summer.

  (2) Glacier melt. In the case of seasonal snow runoff volume, winter precipitation is most important. In the case of glacier melt volume, it is summer temperature[16].
- Inconsistency of the Indus based on the record from Besham, has varied from approximately 85 to 140 percent of the period of record average is 60 MAF [17].
- The wide diversity of hydrologic systems in the mountain basins complicate the problem of transmitting stream flow timing and volumes to a uniform climate change [18].
- The mountain headwaters of the Indus River contribute nearly 60 percent of the mean annual total flow of the river, with about 80 percent of this volume entering the river system during the summer months of June–September [19].

1.6 Annual Hydrograph

The Besham hydrograph, reflecting the merged contributions of all upstream sub-basins shows a seasonal peak in July, supposed to represent peak snowmelt, but instead of beginning a recession phase at that point, has a secondary, slightly lesser peak in August. This is supposed to represent the glacier melt component of the annual stream flow. Following this second peak, the expected exponential recession curve arises[20].

Figure 1.1 Hydrograph Showing Mean Monthly Runoff per Year at Besham

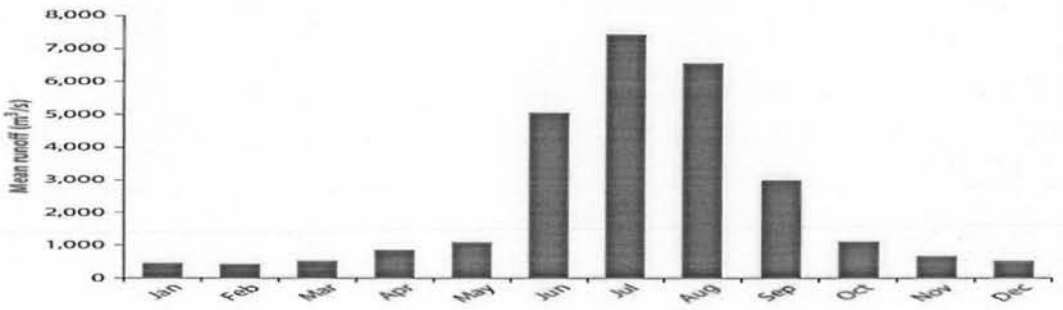

1.7 Climatic Setup

The Karakoram-Himalayas events two distant hydro meteorological setting. Firstly, the Mountainous Snow fed regions of Karakoram and Kashmir. Secondly, the cold parched regions of the Ladakh mountain ranges several glaciers in the locality are influenced by humid environment in the summers (June to September) with an onset of snow fall in the winters and monsoon (November to April) but the characteristic of summer monsoon the Himalayas is absent in the Karakorum range [21].

The major source of regional precipitation is of weak concentration during spring and winter, caused by westerly circulation. These westerlies contribute about two thirds of high-altitude snowfall in the Karakoram. There are two major sources of precipitation in the Indus Basin. The main source in terms of total amounts of precipitation delivered is probably the monsoon, getting storm system from the south. These storms are limited in time from late July through September. They deliver heavy precipitation to the Front Ranges and Main Himalaya [22].

1.8 Literature Review

Pakistan is like many countries in the central Asian region comprises of extensive high mountains juxtaposed with lowlands the mountains provide the principal sources of water supply for large population living in the nearby plains. Hilly areas, with their characteristic glaciers cover and snow, have long been recognized as special hydrological environments receiving relatively heavy precipitation [23].

Archer discussed in 2003 that water resources are more important due to climate variability or socioeconomic factors play an important role in the Upper Indus Basin. The basin was divided into 3 regions: snow fed, glacier fed and rainfall-dependent regions. By analyzing past climate trends, the contribution of 3 regions in river Indus has no significant variation due to climate variability. But evidence indicates that variations are more related to growing socioeconomic culture of the region [24].

Increase in temperature cause a rise in the moisture holding ability of air that leads to more precipitation creating more intense precipitation events. Changing in the climate models are resulting in dry areas becoming drier and wet areas becoming wetter. So with increase in temperature more precipitation events happen as rain rather than snow leading to flood risks in the plain areas [25].

K. Hewitt discussed in 2005 that the climatic inversion of glaciers in Karakoram ranges. The impact of various cyclonical storm and increasing precipitation on glacial extension. In addition the "elevation effect" on glacial melting with solar energy and temperature was also discussed [26].

1.9 Introduction of Remote Sensing

Remote sensing is science and art of getting information about object without getting in contact with the object [27].

Remote sensing is done with satellites sensors, aircrafts etc. and it has tremendous application areas. Recently, Cryosphere research using remote sensing has gained specific importance due to global climate change. Snow cover estimation using in-situ observations is a difficult task, using Remote sensing data snow cover can be estimated with high-level accuracy ensuring wide statistical interpretations covering a large areal extent along with less time constraints [28].

Snow is described by high degree of variability which warrants mapping at finer temporal resolution unlike glacier. The terrain climate and extent of snow cover renders traditional station based insitu observation futile at regional scale. Alternatively, the RS (remote sensing) based techniques and tool has proved very useful in mapping snow from space. The contribution of insitu data however in validation of snow products generated through remote sensing methods and improvement of snow mapping algorithm is essential. (ICIMOD) [29].

1.10 Study Area

Total area of Hunza river basin is 15786 km^2. Which is located in the high-level mountainous region of central karakoram with almost 4453km^2 of catchment area at an elevation more than 5000m [29].

In summer 30 percent cover with snow and increases almost 80 percent in winter. Mean flow of Hunza river is 323m^3 (i.e. 742 mm of water depth equivalent) gauged at Dainyor bridge according to the almost 40 years 1966-2008 flow record of the SWHP-WAPDA [30].

Map 1.2 Hunza Basin Catchment Map

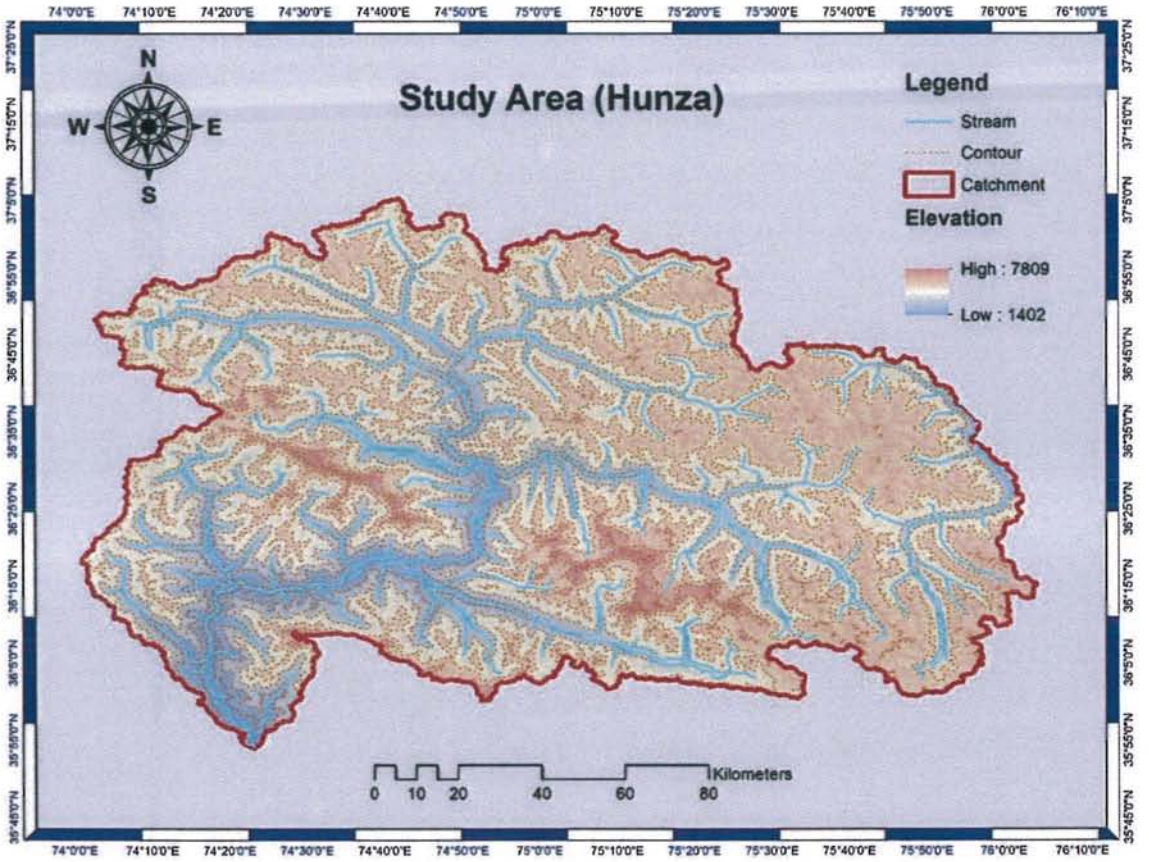

1.11 Physical Characteristics of Hunza River Basin

Physical Characteristics	Description
Catchment Area	15789 km^2
Glacier	2868 km^2

Latitude	35°45` to 37°25`
Longitude	74°00` to 76°10`
Discharge Gauging Station: Mean Runoff (1966 to 2008)	Danyor Bidge 323 m^3/s

1.12 Data Source

Pakistan meteorological department was tasking daily basis temperature (Max & Min) and rainfall data of Hunza meteorological station. MODIS snow product were chosen to calculate the snow cover percentage in our study area. Aqua and Terra Snow cover 8-Day L3 Global 500m Grid "MOD10A2" Used for this study contains data fields for maximum snow cover extent over an 8-day repeated period and has a resolution of approximately 500m converting the Hunza River Basin completely. A data set of 2024 processed MOD10A2 image available [31].

1.13 Study Objectives

The climate variation with in the Hunza River.

The sessional and annual relationship between snow cover mean temperature & rainfall in the Hunza, river basin [32].

CHAPTER 2

METHODOLOGY AND PROCESSING

2.1 GENERAL

The geographical area considered for this study is Hunza River Basin situated in the northern areas (Karakoram region) of Pakistan. It ranges from 74.5° - 76.5°E in Longitude, and 35.2° - 36.38°N in Latitude. To estimate the Snow Cover Area of Hunza firstly the area was identified on Google Earth Pro for displaying the satellite image of study area. Then the catchment area of Hunza was also identified by using software (ArcGIS). GIS is a (geographic information system) for working with geographic information and maps. It's used for creating and using maps; compiling geographic data; analyzing mapped information; sharing and discovering geographic information; using maps and geographic information in a range of applications; and managing geographic information in a database [33]. ArcGIS is available at three functional levels consisting of Arc View that focuses on comprehensive data use, mapping, and analysis; Arc View consist of ArcMap, ArcCatalog and Arc Toolbox, secondly Arc Editor which adds advanced geographic editing for shape files and geo-database, and creation of data, and thirdly Arc Info that is complete GIS desktop, containing wide range GIS functionality [34].

The methodology includes the following steps.

2.2 Remote Sensing

Remote Sensing of Snow is entirely dependent upon reflectance patterns in different bands. Snow has the property in "Visible Region of EM Spectrum: Highly Reflective" "Infrared Region of EM Spectrum: Highly Absorptive". Using this property data when observed in visible region will indicate snow while in infrared it will show the area where snow is absent [35].

Using this property NDSI (Normalized difference Snow Index) is formed

$$NDSI = (V-IR) / (V+IR)$$

V=Visible band IR= Infrared Band

Latitude	35°45` to 37°25`
Longitude	74°00` to 76°10`
Discharge Gauging Station: Mean Runoff (1966 to 2008)	Danyor Bidge 323 m^3/s

1.12 Data Source

Pakistan meteorological department was tasking daily basis temperature (Max & Min) and rainfall data of Hunza meteorological station. MODIS snow product were chosen to calculate the snow cover percentage in our study area. Aqua and Terra Snow cover 8-Day L3 Global 500m Grid "MOD10A2" Used for this study contains data fields for maximum snow cover extent over an 8-day repeated period and has a resolution of approximately 500m converting the Hunza River Basin completely. A data set of 2024 processed MOD10A2 image available [31].

1.13 Study Objectives

The climate variation with in the Hunza River.

The sessional and annual relationship between snow cover mean temperature & rainfall in the Hunza, river basin [32].

NDSI is core logic behind snow cover extraction using satellite data. It can be generated using Model Builder in any GIS or RS software capable of MMC (Model Management Component) [36].

2.2.1 Satellites for Remote Sensing

Different satellite sensors can be used for snow cover mapping, MODIS, TIROS, and LANDSAT etc. Different sensors provide data according to their specifications requiring different type of classification or snow cover extraction algorithms. Landsat 7 ETM+ imagery can be used for snow cover, but the temporal resolution of Landsat is 16-days [37].

Among various data sets MODIS Snow Cover Product proved to be easily accessed, approached, and processes able data ensuring high accuracy and quality. (ICIMOD) [38].

2.3 MODIS for Remote Sensing

MODIS is a key instrument aboard first NASA EOS satellite, called Terra, launched on December 18, 1999 and on the Aqua satellite, launched on May 3, 2002. Due to continuous coverage of the MODIS (Moderate resolution Imaging Spectroradiometer) the whole picture of Globe can be obtained in "two" days [39] .

2.3.1 Characteristics of MODIS

MODIS features are designed to detect a wide range of the electromagnetic energy, and measure at three different spatial levels, it takes measurements on 24/7 basis; and it has a wide field of view. Due to comprehensive and continual coverage MODIS offers a complete global electromagnetic picture in two days. "MODIS's frequent coverage complements other imaging systems such as Landsat's Enhanced Thematic Mapper Plus, which reveals the Earth in finer spatial detail, but can only image a given area once every 16 days— too infrequently to capture many of the rapid biological and meteorological changes that MODIS observes" [40].

These MODIS instruments are designed to take measurements in spectral regions that have been used in previous satellite sensors. MODIS is continually adding to existing knowledge by extending data sets collected by heritage sensors series such as the National Oceanic and Atmospheric Administration's (NOAA) Advanced Very High Resolution Radiometer (AVHRR), used for meteorology and monitoring sea surface temperature, sea ice, and vegetation; the Coastal Zone Color Scanner (CZCS) and the Sea viewing Wide Field of View Sensor used to monitor

ocean biological activity; Landsat, used to monitor terrestrial conditions; and NOAA's High Resolution Infrared Radiation Sounder (HIRS), used to observe atmospheric conditions. By extending these data sets, MODIS promotes the continuity of data collection essential for understanding both long- and short-term change in the global environment [41].

2.3.2 Spectral Properties of MODIS

Its detectors measure 36 spectral bands between 0.405 and 14.385 μm, and it acquires data at three spatial resolutions. The automated MODIS snow-mapping algorithm uses at-satellite reflectance's in MODIS bands 1 (0.659 μm), 2 (0.865 μm), 4 (0.555 μm) and 6 (1.64 μm). Snow has two properties: high reflectance in the visible (MODIS band 4) and low reflectance in the short-wave infrared (MODIS band 6). The Normalized Difference Snow Index (NDSI) using bands 4 and 6 makes snow detection possible [42].

2.3.3 Temporal and Spatial resolution of MODIS

MODIS has swath width of 2,330 km The MODIS snow product suite is composed of products covering a range of spatial and temporal resolutions, from 500 m to 0.25°, and from swath to daily, to 8-day to monthly. All products provide fractional snow cover, and snow albedo is provided in the 500-m resolution products, and all have been validated to stage 1 or 2. The overall absolute accuracy of the 500-m resolution products is ~93%, varying by land cover and snow condition. The snow products are used by climatologists, and by modelers both as input to hydrological models, e.g., to develop snow-cover depletion curves, and to compare with output. Following table indicates spatial properties and spectral bands of MODIS [43].

Table 2.1 Spectral Bands of MODIS

Band	Spatial resolution	Bandwidth*	Band	Spatial resolution	Bandwidth*
1	250m	620-670	19	1km	915-965
2		841-876	20		3.660-3.840
3	500m	459-479	21		3.929-3.989
4		545-565	22		3.929-3.989
5		1230-1250	23		4.020-4.080
6		1628-1652	24		4.433-4.498
7		2105-2155	25		4.482-4.549
8	1km	405-420	26		1.360-1.390
9		438-448	27		6.535-6.895
10		483-493	28		7.175-7.475
11		526-536	29		8.400-8.700
12		546-556	30		9.580-9.880
13		662-672	31		10.780-11.280
14		673-683	32		11.770-12.270
15		743-753	33		13.185-13.485
16		862-877	34		13.485-13.785
17		890-920	35		13.785-14.085
18		931-941	36		14.085-14.385
* Bands 1 to 19 are in nm; Bands 20 to 36 are in μm					

2.3.4 MODIS Snow Cover Product

The MODIS snow algorithm produces maps of snow extent using reflective and thermal data from the MODIS instrument at the swath level. Snow extent products are generated at several levels from a swath, about 2030 x 2330 km coverage, at 500 m resolution to daily composited global Climate Modelling Grid (CMG) products at 0.05-degree resolution [44].

Table 2.2 MODIS Snow Cover Product

Data Type	Product level	Nominal Data Array Dimensions	Spatial Resolution	Temporal Resolution	Map Projection
MOD10_L2	L2	1354km x 2000km	500m	Swath scene	None
MOD10L2G	L2G	1200km x 1200km	500m	Day of multiple coincident swath	Sinusoidal
MOD10A1	L3	1200km x 1200km	500m	day	Sinusoidal
MOD10A2	L3	1200km x 1200km	500m	eight day	Sinusoidal
MOD10C1	L3	360° by 180° (global)	0.05° by 0.05°	day	Geographic
MOD10C2	L3	360° by 180° (global)	0.05° by 0.05°	eight day	Geographic
MOD10CM	L3	360° by 180° (global)	0.05° by 0.05°	month	Geographic

2.3.5 MODIS 8 Day Product

Snow cover in our project is mapped as maximum snow extent at interval of eight days.

Start: First day of the year.

End: Extend into the next year.

An eight-day compositing period was chosen because that is the ground track repeat period of the Terra platform. The last eight-day period of a year extends into first few days of the next year.

The product can be produced with two to eight days of input.

Issues: There may not always be eight days of input, because of various reasons, so the user should check the attributes to determine what days observations were obtained or were missing in a period [45].

2.3.6 MODIS Projection System

In the sinusoidal projections, areas on the data grids are proportional to the same areas on the Eart and distances is corrected along the central meridian and all parallels. Shapes are gradually distorted away from the central meridian or near the poles. Finally the data are neither conformal, perspective nor equidistant (USGS 2000) [46].

2.3.7 MODIS Data Representation

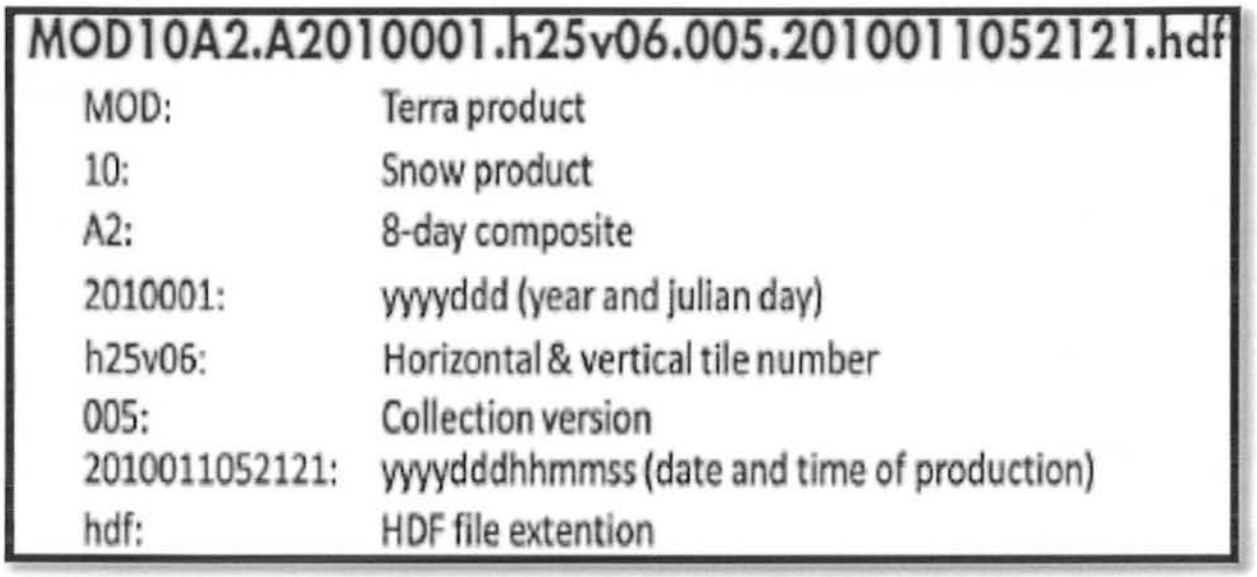

Figure 2.1 MODIS Data Representation

2.3.8 MODIS Summary

MODIS Features (Table 2.3)

Orbit	705 km, 10:30 a.m. descending node (Terra) or 1:30 p.m. ascending node (Aqua), sun-synchronous, near-polar, circular
Scan Rate	20.3 rpm, cross track
Swath Dimensions	2330 km (cross track) by 10 km (along track at nadir)
Telescope	17.78 cm diam. Off-axis, afocal (collimated), with intermediate field stop

Size	1.0 x 1.6 x 1.0 m
Weight	228.7 kg
Power	162.5 W (single orbit average)
Data Rate	10.6 Mbps (peak daytime); 6.1 Mbps (orbital average)
Quantization	12 bits
Spatial Resolution	250 m (bands 1-2) 500 m (bands 3-7) 1000 m (bands 8-36)
Design Life	6 years

2.3.9 Data Collection

Moderate Resolution Imaging Spectroradiometer (MODIS) snow product was utilized to estimate the snow cover of Hunza Basin. Cloud free satellite images of the year 2003-2011 of Hunza should be obtained [7]. The MODIS snow cover algorithm works on the principle of high reflectance of snow in visible band 6 and band 4, likewise these two bands are used to calculate NDSI. Data for daily precipitation, maximum temperature, and minimum temperature over the period of Hunza considered in monitoring the snow cover [6].

2.4 Modis Snow Tool Operation

Data set is prepared by downloading Images from MODIS server. Aqua & Terra images were separately downloaded and arranged in a folder specified in MODIS Snow tool. MODIS snow tool incorporates automated processing and report generation. First step after downloading the data set is to specify all images a space in MST directory where data can be processed. A Parameter file needs to be created in MODIS tool based upon which coordinate system and projection Parameters will be assigned to Tiles. Once the parameter file is created, we would Reproject MODIS Tile Product that transforms images into a defined projection system based on a parameter file specified [47].

Next step involves converting GeoTiff images into HDR format. TIFF format is the most popular and versatile raster data format in the world today. HDR stands for hierarchical data format, is the only format process able in MODIS Snow tool. In Next phase involves combining Aqua & Terra

Products, like mosaicking. Once mosaicking is done cloud filtering is carried out in following three ways.

- ✓ Temporal Filter
- ✓ Spatial Filter
- ✓ Temporal Analyzer

Temporal Filter & Temporal analyzer work on the principle "Take three consecutive images and assign the middle image cloud covered pixel the average values of other two image pixels", so the condition for this is to use at least three images.

Spatial Filter works on the principle that spatial window of specific Kernel is applied e.g.; a window of 4*4 will be assigning the pixel values on basis of surrounding four pixels. Once filtering is completed, we generated snow cover by region of interest [48].

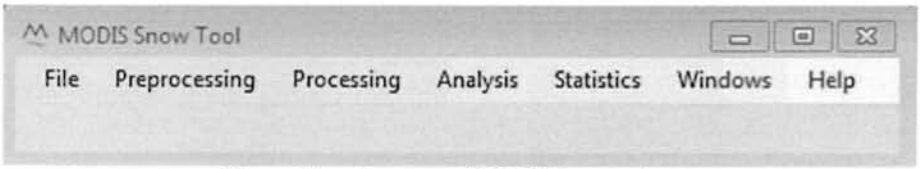

Figure 2.2 main manu of MODIS Snow tool

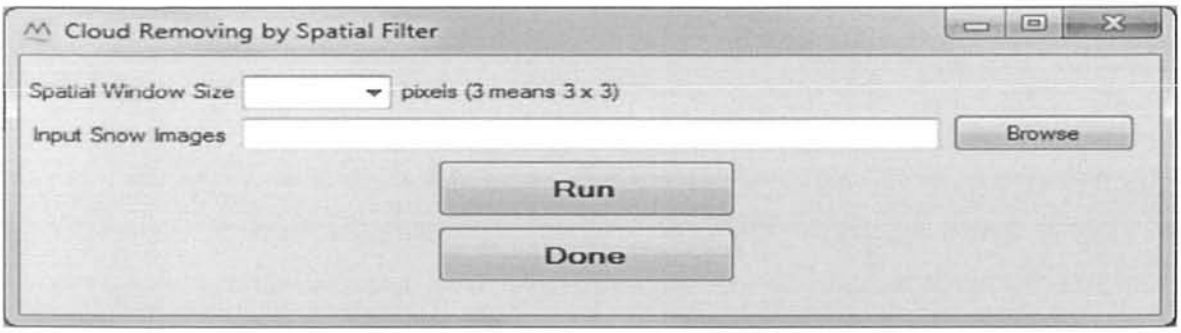

Figure 2.6 Spatial Filtering

2.4.5 Temporal Analysis Filtering

- From **main menu**, select **Processing >> Remove Cloud by >> Temporal Analysis**. A **Cloud Removing by Temporal Analysis** window will appear.
- The **C:\MODIS\data\Filter_Spatial** will be used as the input directory for temporal analysis. **Browse** for an input file **MOD10A2_2000057_lt.Maximum_Snow_Extent__sf7x7.**hdr from the **C:\MRT\data\Filter_Spatial folder.**
- . Replace the file name with wildcard character (*) to process all the files in the folder. The input file should resemble **C:\MRT\data\Filter_Spatial\MOD10A2_*_lt.*.hdr**. The program will take advantage of the systematic file names (YYYYDOY) in sequential orders to perform the temporal analysis for multiple files.
- Click **Run** button to implement temporal analysis.
- The output file is named automatically after the input file name followed a suffix **_ta** from this process.

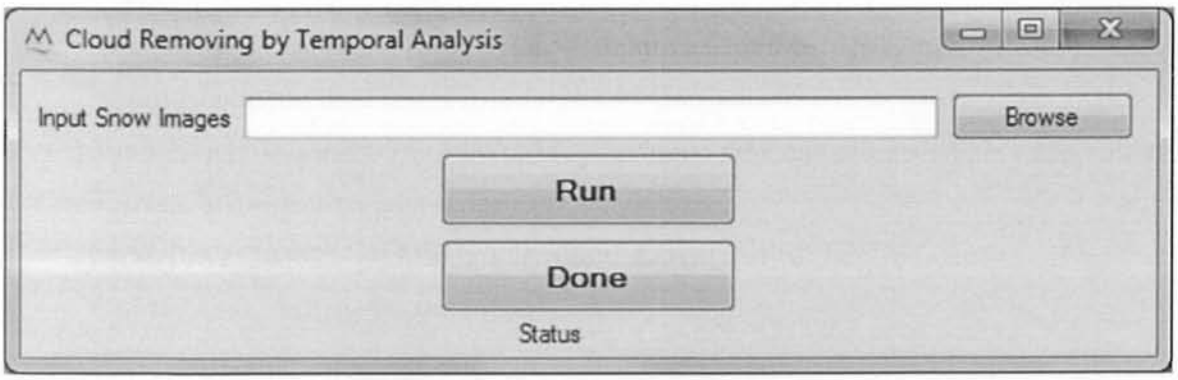

Figure 2.7 Temporal Analysis Filtering

2.5 Outputs of MODIS

Figure 2.8 Snow with Clouds

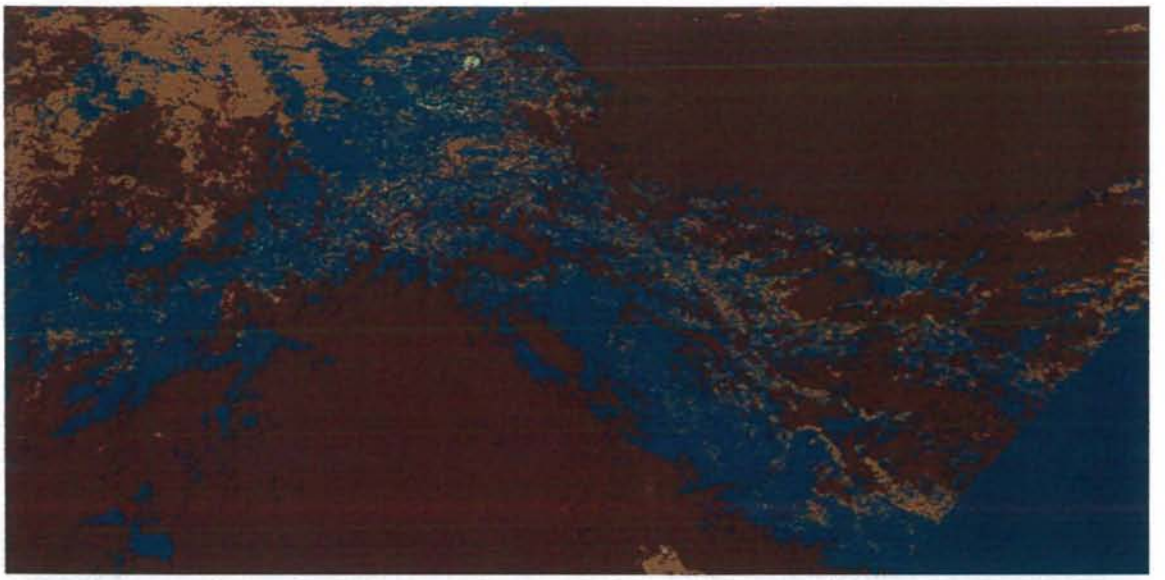

Figure 2.9 Snow Without Clouds (filtered image)

Snow **Clouds** **Land**

Workflow of ArcMap

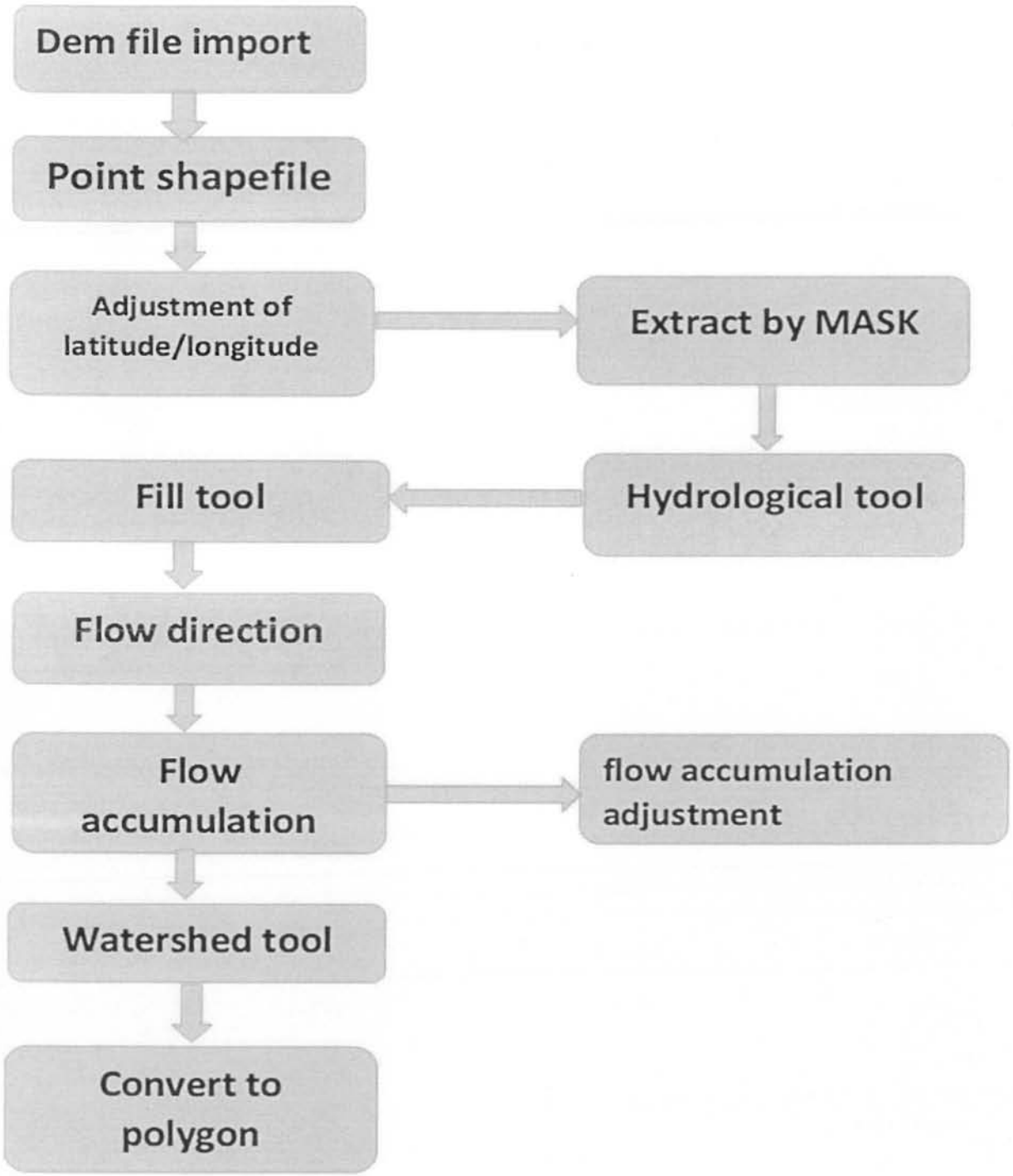

2.6 ArcMap

This section provides an introduction and overview to ArcMap, which is the central application used in ArcGIS. ArcMap is where you display and explore GIS datasets for your study area, where you assign symbols, and where you create map layouts for printing or publication. ArcMap is also the application you use to create and edit datasets [49].

ArcMap represents geographic information as a collection of layers and other elements in a map. Common map elements include the data frame containing map layers for a given extent plus a scale bar, north arrow, title, descriptive text, a symbol legend, and so on [50].

2.6.1 Spatial Analyst Tool

The ArcGIS Spatial Analyst extension provides a rich set of spatial analysis and modeling tools for both raster (cell-based) and feature (vector) data.

The capabilities of Spatial Analyst are broken down into categories or groups of related functionalities. Knowing the categories will help you identify which tool to use. The table at the end of this section lists all the available toolsets with a description of the capabilities offered by the tools in each. It consists of different tools such as density, distance, local, raster calculator, hydrology, or interpolation etc. [51].

2.6.1.1 Hydrology Tool

The hydrologic modeling tools in the ArcGIS Spatial Analyst extension toolbox provide methods for describing the physical components of a surface. The hydrologic tools allow you to identify sinks, determine flow direction, calculate flow accumulation, delineate watersheds, and create stream networks. The image below is of a resulting stream network derived from an elevation model [52].

Using an elevation raster or digital elevation model (DEM) as input, it is possible to automatically delineate a drainage system and quantify the characteristics of the system. The following graphics illustrate the steps involved in calculating a watershed and stream network from a DEM [53].

2.6.1.2 Working of Fill (Tool)

Fills sinks in a surface raster to remove small imperfections in the data. Sinks should be filled to ensure proper delineation of basins and streams. If the sinks are not filled, a derived drainage network may be discontinuous [53].

2.6.1.3 Flow Direction

Creates a raster of flow direction from each cell to its downslope neighbor, or neighbors, using D8, Multiple Flow Direction (MFD) or D-Infinity (DINF) methods.

This tool takes a surface as input and outputs a raster showing the direction of flow out of each cell. If the Output drop raster option is chosen, an output raster is created showing a ratio of the maximum change in elevation from each cell along the direction of flow to the path length between centers of cells and is expressed in percentages. If the Force all edge cells to flow outward option is chosen, all cells at the edge of the surface raster will flow outward from the surface raster [54].

Illustration

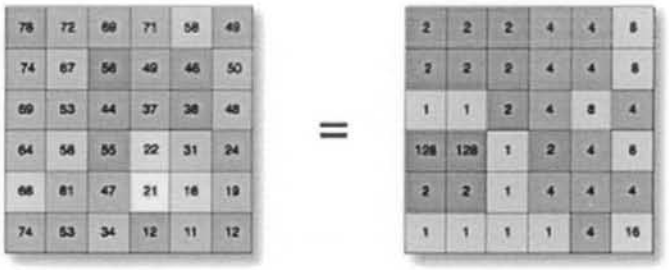

Figure 2.10 Flow Direction

Usage

Output of Flow Direction tool is an integer raster. Values range from 1 to 255.Values for each direction from the center are the following.

32	64	128
16		1
8	4	2

For example, if the direction of steepest drop were to the left of the current processing cell its flow direction would be coded as 16.

The direction of flow is determined by the direction of steepest descent, or maximum drop, from each cell. This is calculated as follows.

maximum drop = change_in_z-value / distance * 100

The distance is calculated between cell centers. Therefore, if the cell size is 1, the distance between two orthogonal cells is 1, and the distance between two diagonal cells is 1.414 (the square root of 2). If the maximum descent to several cells is the same, the neighborhood is enlarged until the steepest descent is found.

- If a cell is lower than its eight neighbors, that cell is given the value of its lowest neighbor, and flow is defined toward this cell. If multiple neighbors have the lowest value, the cell is still given this value, but flow is defined with one of the two methods explained below. This is used to filter out one-cell sinks, which are considered noise.
- If a cell has the same change in z-value in multiple directions and that cell is part of a sink, the flow direction is referred to as undefined. In such cases, the value for that cell in the output flow direction raster will be the sum of those directions. For example, if the change in z-value is the same both to the right (flow direction = 1) and down (flow direction = 4), the flow direction for that cell is 1 + 4 = 5. Cells with undefined flow direction can be flagged as sinks using the Sink tool.
- If a cell has the same change in z-value in multiple directions and is not part of a sink, the flow direction is assigned with a lookup table defining the most likely direction. See Greenlee (1987).
- The output drop raster is calculated as the difference in z-value divided by the path length between the cell centers, expressed in percentages. For adjacent cells, this is analogous to the percent slope between cells. Across a flat area, the distance becomes the distance to the nearest cell of lower elevation. The result is a map of percent rise in the path of steepest descent from each cell.

- When calculating the drop raster in flat areas, the distance to diagonally adjacent cells (1.41421 * cell size) is approximated by 1.5 * cell size for improved performance [55].

2.6.1.4 Flow Accumulation

Creates a raster of accumulated flow into each cell. A weight factor can optionally be applied.

Illustration

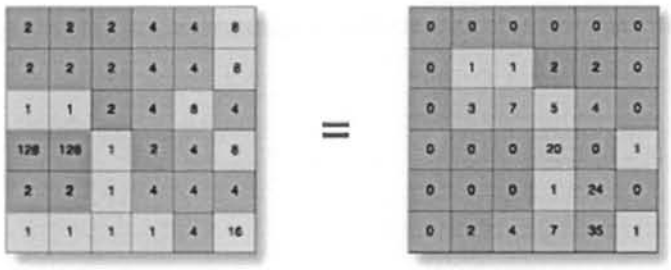


```
Flow_Acc = FlowAccumulation(Flow_Dir)
```

Figure 2.11 Flow Accumulation

Usage

- The result of Flow Accumulation is a raster of accumulated flow to each cell, as determined by accumulating the weight for all cells that flow into each downslope cell.
- Cells of undefined flow direction will only receive flow; they will not contribute to any downstream flow. A cell is considered to have an undefined flow direction if its value in the flow direction raster is anything other than 1, 2, 4, 8, 16, 32, 64, or 128.
- The accumulated flow is based on the number of cells flowing into each cell in the output raster. The current processing cell is not considered in this accumulation.
- Output cells with a high flow accumulation are areas of concentrated flow and can be used to identify stream channels.
- Output cells with a flow accumulation of zero are local topographic highs and can be used to identify ridges.

- If the input flow direction raster is not created with the Flow Direction tool, there is a chance that the defined flow could loop. If the flow direction does loop, Flow Accumulation will go into an infinite loop and never finish.
- The Flow Accumulation tool does not honor the Compression environment setting. The output raster will always be uncompressed.

2.6.1.5 Watershed

A watershed is the upslope area that contributes flow—generally water—to a common outlet as concentrated drainage [56]. It can be part of a larger watershed and can also contain smaller watersheds, called sub basins. The boundaries between watersheds are termed drainage divides. The outlet, or pour point, is the point on the surface at which water flows out of an area. It is the lowest point along the boundary of a watershed [57].

Figure 2.12 Watershed of Hunza Basin

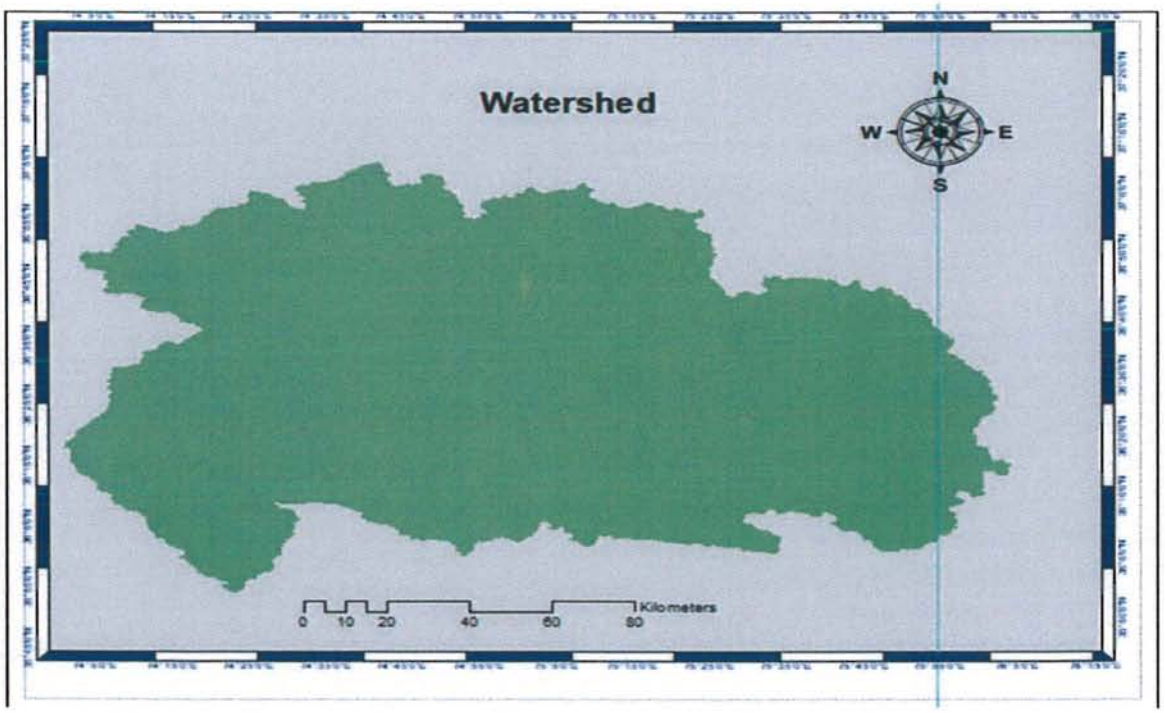

Outputs of ArcMap

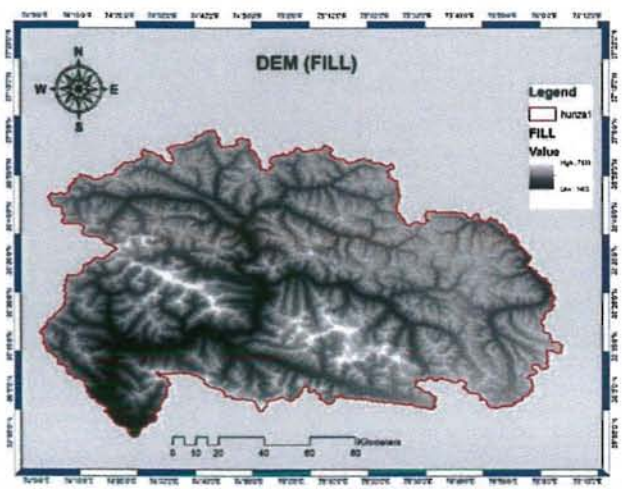

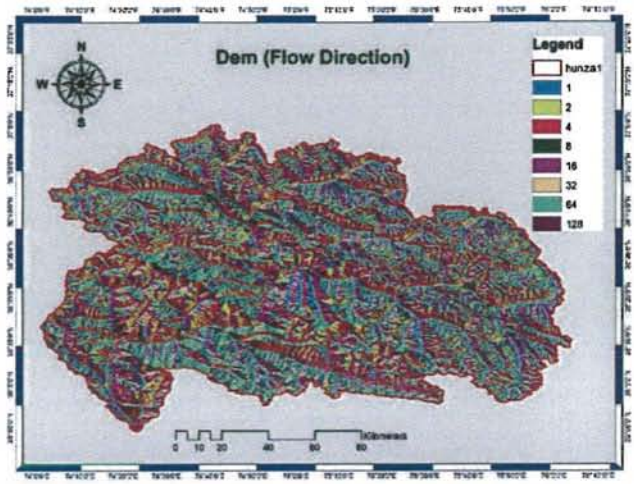

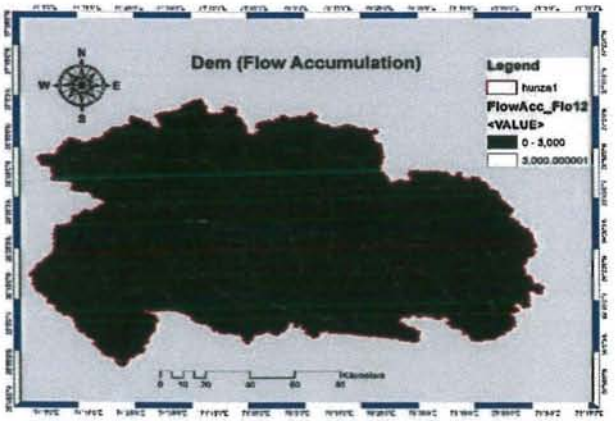

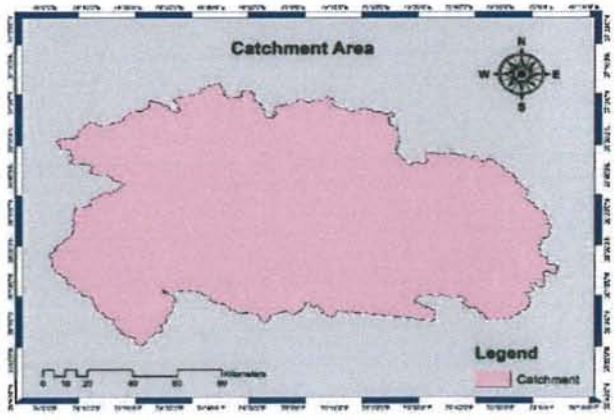

Chapter 3

Results and Discussions

We had calculated snow cover by using MODIS snow tool. MODIS data was available from 2003 to 2011. Calculated the average, maximum, minimum trend also calculated winter and summer trend and correlate with temperature rainfall. Temperature rainfall data was available from 2007 to 2011.

Table 3.1 Areal Extent of Snow Cover (km^2)

Years	JFM	AMJ	JAS	OND
2003	12304.81	11838.69	7768.37	11776.73
2004	13311.32	11224.01	8584.004	11731.64
2005	13455	11676.61	7910.5	11975.7
2006	12131.22	10350.15	76.38.44	11744.63
2007	12180.44	9864.744	7417.668	9683.489
2008	13844.27	9892.578	7548.547	11637.91
2009	13844.27	11545.56	8644.587	132792.3
2010	11938.69	11622.33	8359.594	9777.312
2011	12421.6	10114	7640.548	11135.61

Table 3.2 Average Seasonal Temperature of Hunza Basin (^{o}c)

Year	DJFM	AMJ	JAS	ON
2007	-1.58	12.29	15.12	5.30
2008	-3.08	11.99	13.47	5.19
2009	-2.63	9.10	14.73	3.32
2010	-1.70	9.37	14.04	4.69
2011	-2.24	11.59	15.24	4.97

Table 3.3 Total Seasonal Rainfall of Hunza Basin (mm)

Year	DJFM	AMJ	JAS	ON
2007	306.3	139.2	74.2	36.2
2008	171.7	123.9	159.7	36.1
2009	292.6	236.4	134,3	48.9
2010	229.5	217.8	336.7	43.8
2011	407.5	162.8	300	54.3

3.1 Maximum Snow Cover Trend (2003-2011)

Observation was made in maximum snow cover with decreasing trends. For the duration of 9 years, Point Value of Maximum Snow Cover was calculated and plotted.

Maximum Snow Cover in 2003 was above 14050km^2 then snow reach at 14781 in two years. However, it decreases and reach at 14000 in next 3 year and then increase at 14500 and next two year it decreases and reach at 13430.

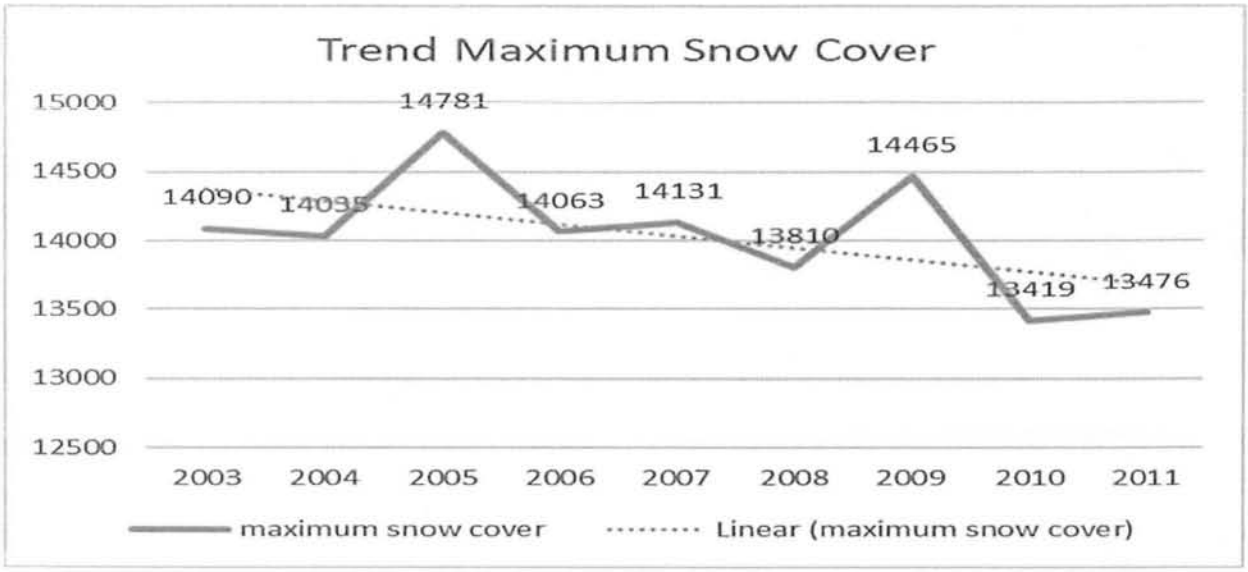

Minimum Snow Cover Trend (2003-2011)

The values of minimum snow cover of 9 years were compared, and it is concluded that minimum snow cover is on almost same trend in past 9 years that shows that are snow cover in summer retained a stability.

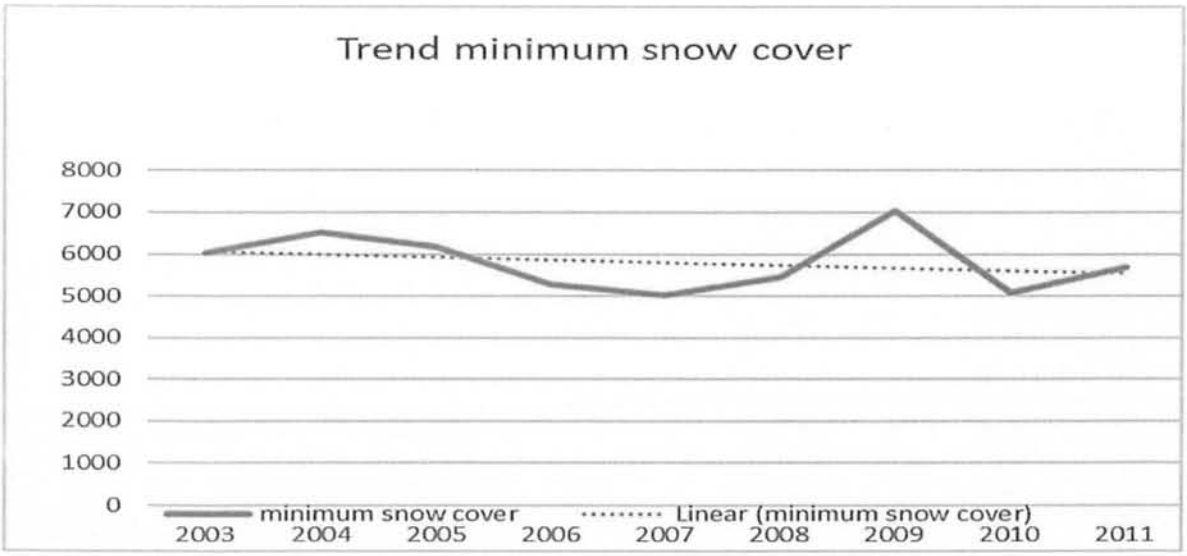

Average snow cover

Our average snow cover shows a juxtaposed behavior showing alternative episodes of increment and decrement 2007 was the year with least minimum snow cover.

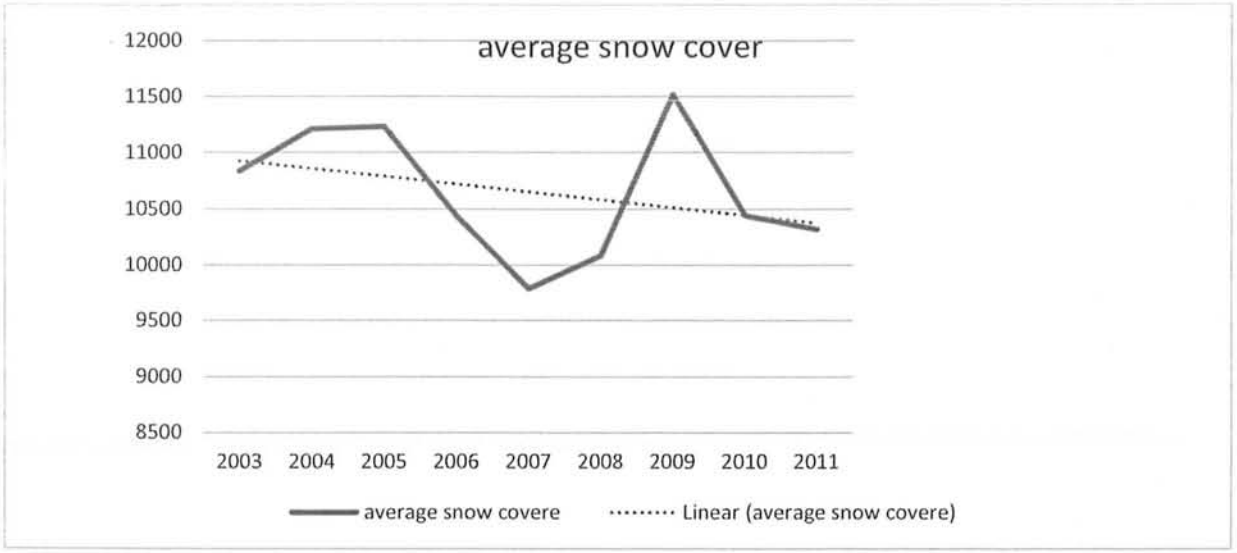

Winter Snow Cover

No, significant changes were observed during our 9-year dataset. Results are in agree with the various research on Karakorum region which shows stabilizing glaciers in this part of word despite of global retreat of glaciers.

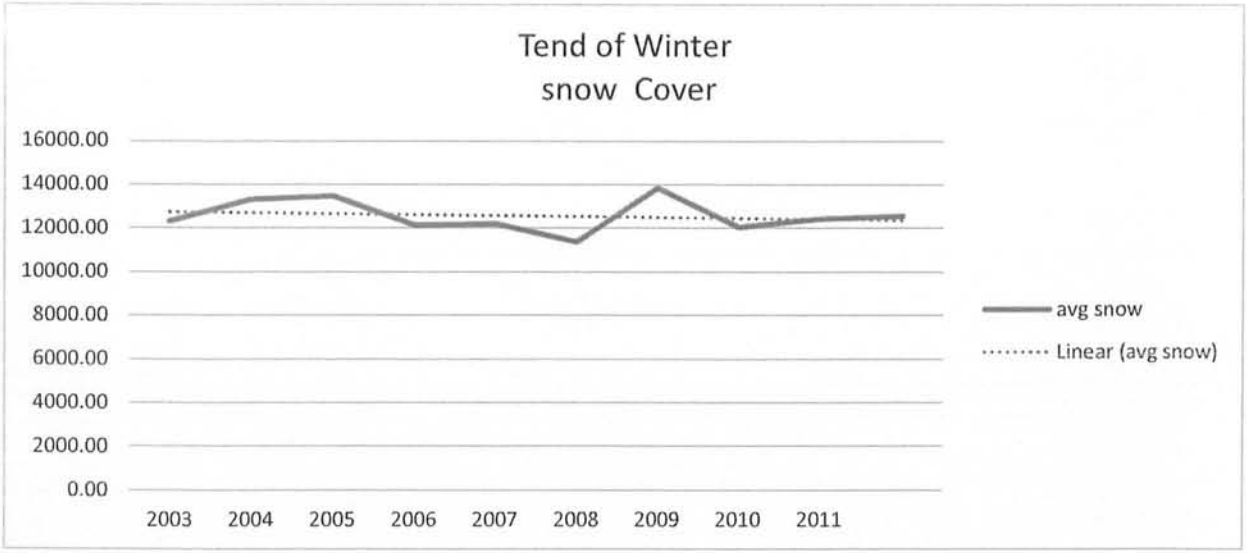

Summer snow cover

Our trend line is in harmony with previous winter snow results, no change in summer snow cover is present in analyzed data. Despite of increase in global temperatures, no considerable effect is seen over our summer snow cover.

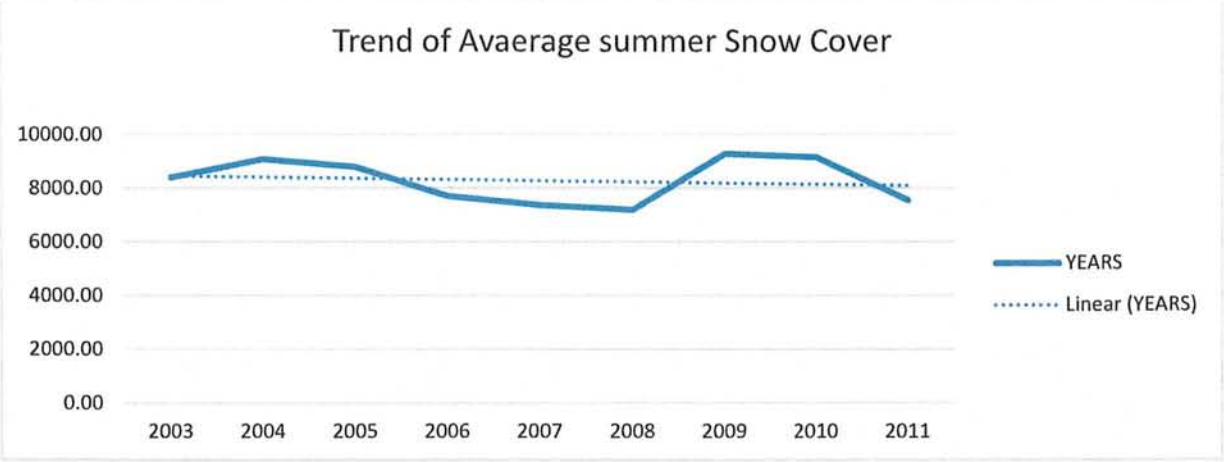

Average Snow Cover V/S Average Temperature

Empirical formula of SC and temperature exist in our analysis, snow cover is inversely proportional to the mean temperature .2011 summer was out of context year with least snow cover area despite of no major surge in temperature. The reason can be lack of data on altitudes.

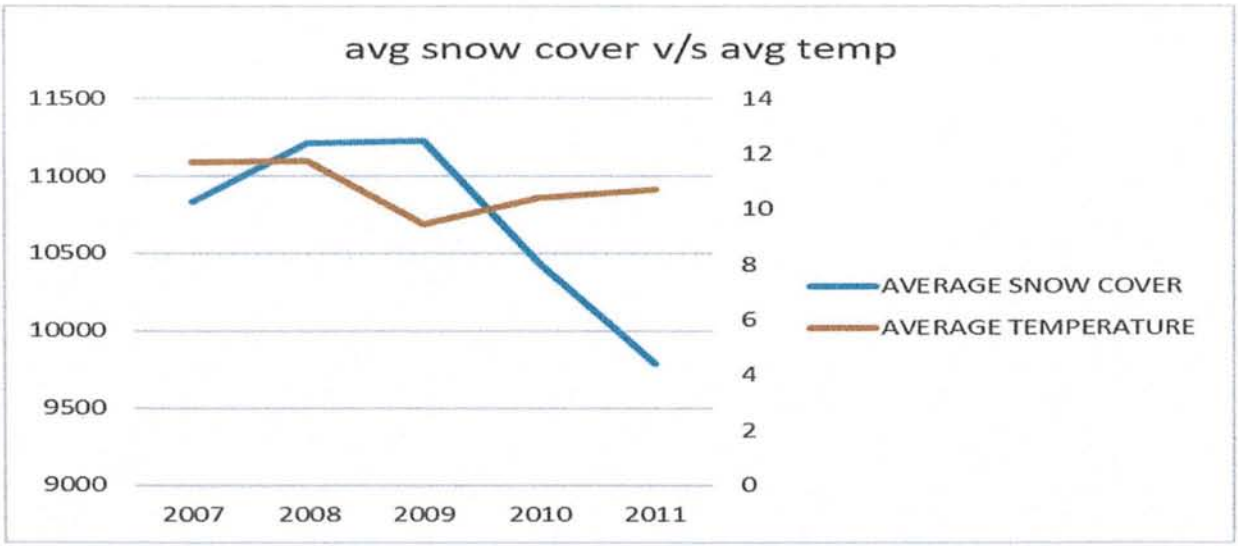

Avg Summer Snow Cover V/S Avg Temp

In 2007 to 2008 temp were higher and the snow cover were at lower note and the next consecutive three years the temperature was at lower note approaching near 20°C and snow cover were at higher note and approaches 9000km^2.

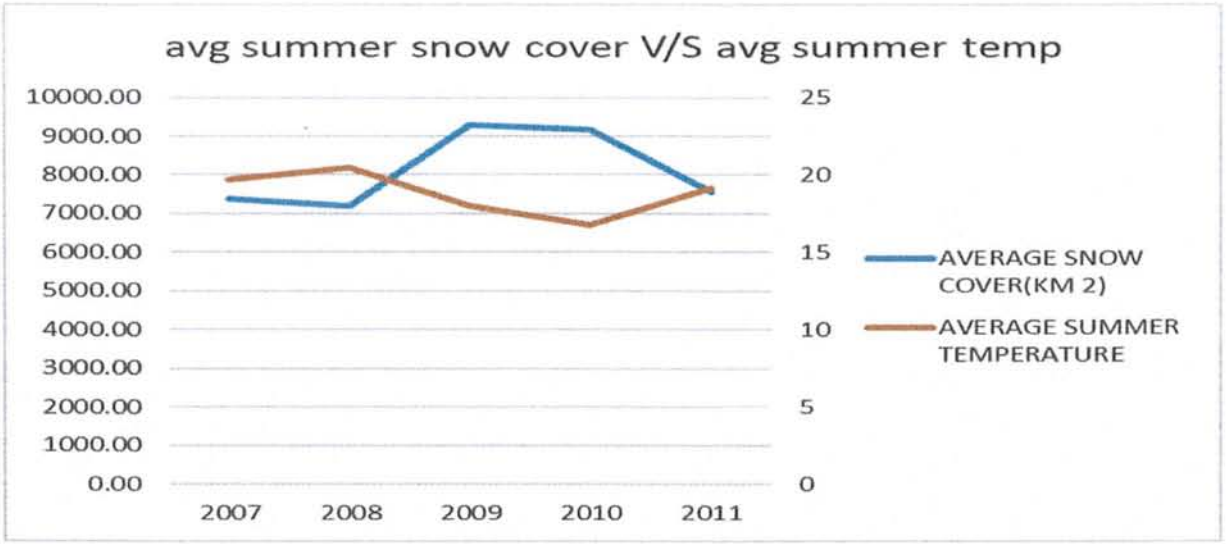

Avg Winter Snow Cover V/S Avg Temp

No, proper relation exist between our analysis data of average winter temperature and average winter snow cover.

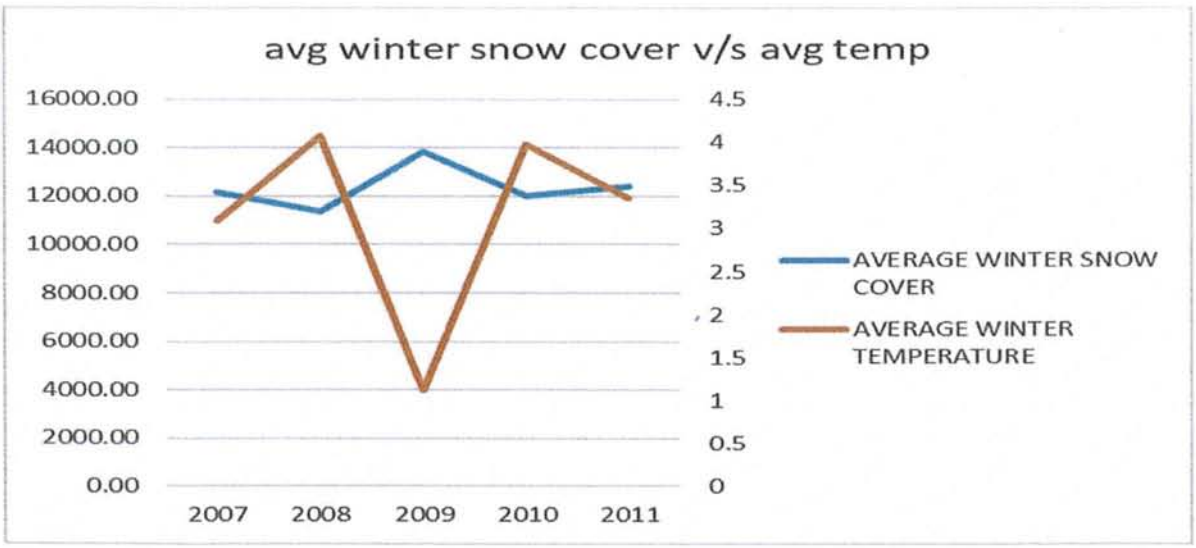

3.2 RAINFALL COMPARISON TO SNOW COVER

The data of temperature is insufficient for any fruitful outcome of the analysis, so effort was made to relate snow cover with rainfall. The data of daily basis was taken from Pakistan Meteorological Department. A small set of data from 2007-2011 was available.

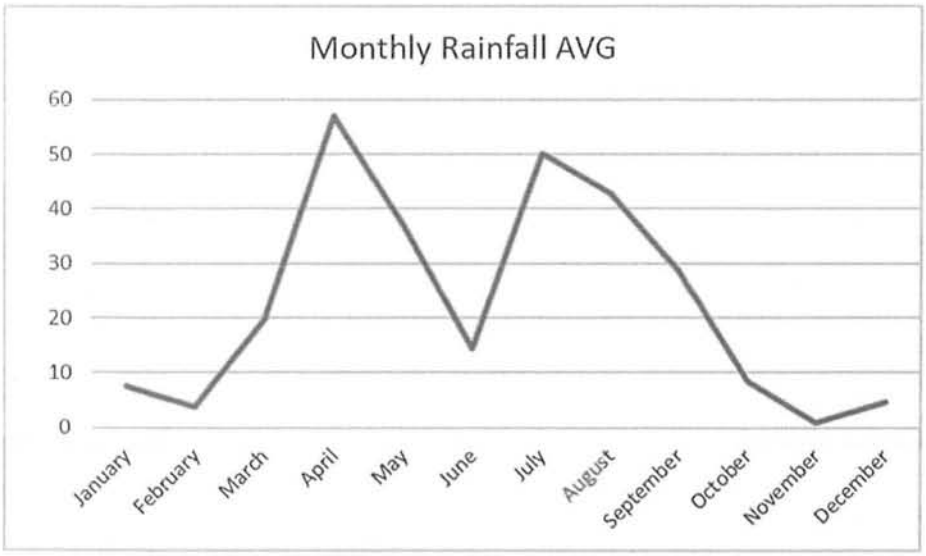

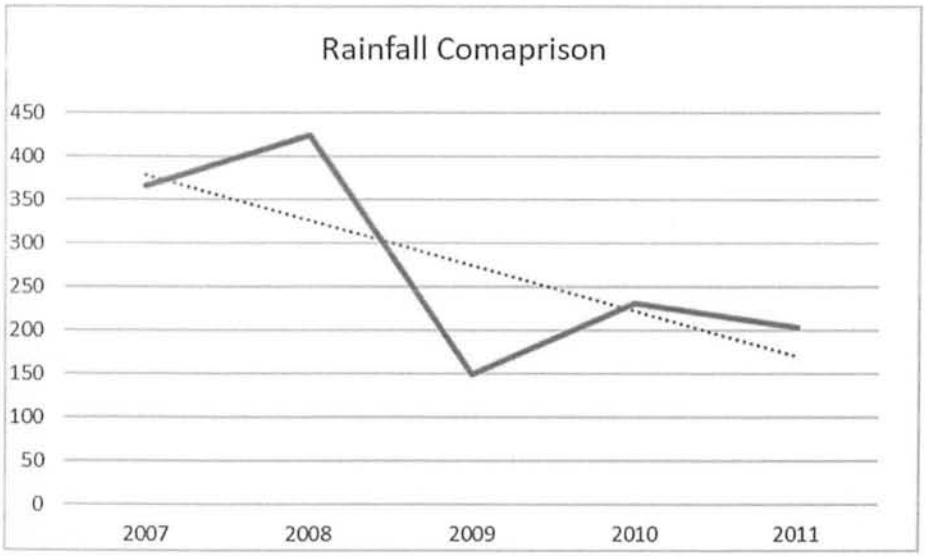

During the 5 years, rainfall shows a decreasing trend with 2008 experiencing most count and 2009 with least count.

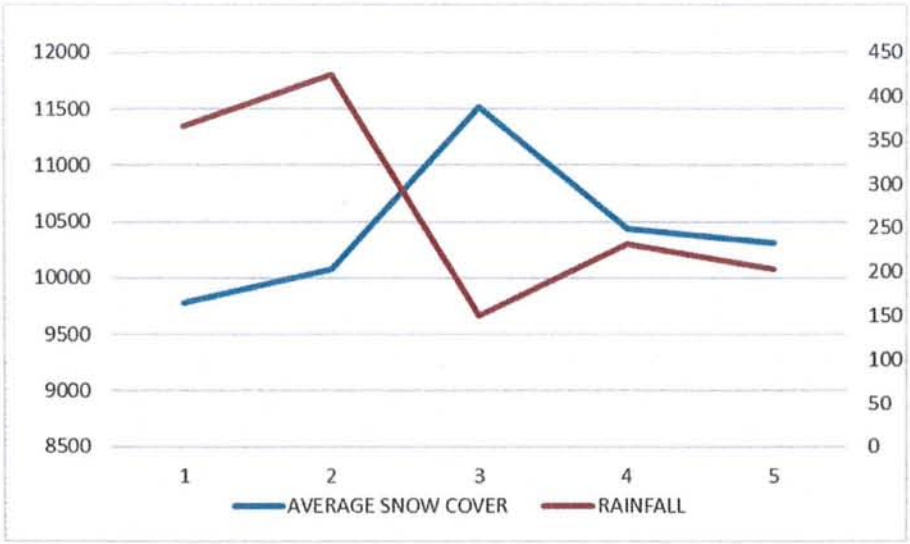

2007 and 2008 were the wettest year with least snow cover and 2009 experienced greater snow cover with least rainfall. It is proposed that more rainfall is reflective of snowline at greater elevation and less rainfall is indicative of much lower snowline w.r.t ASML.

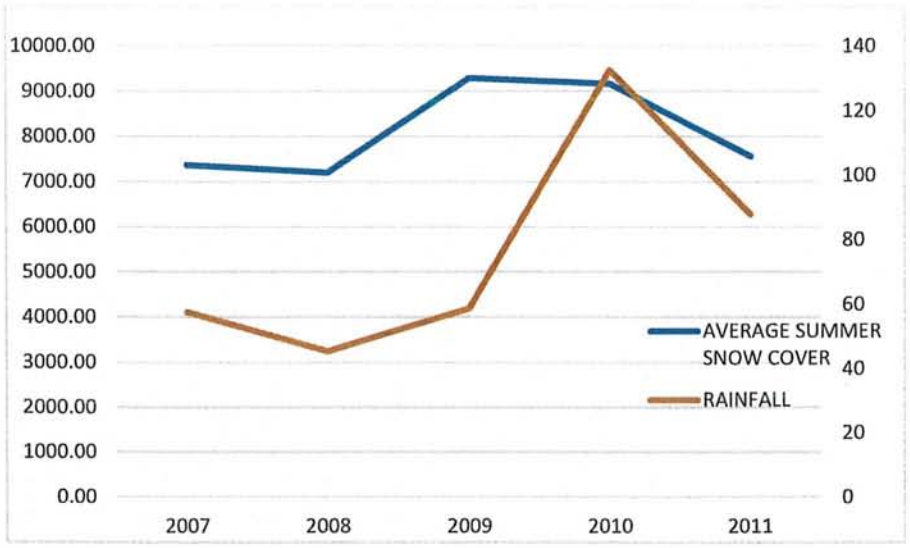

No relation exists for rainfall and summer snow cover. The reason can be lack of data duration.

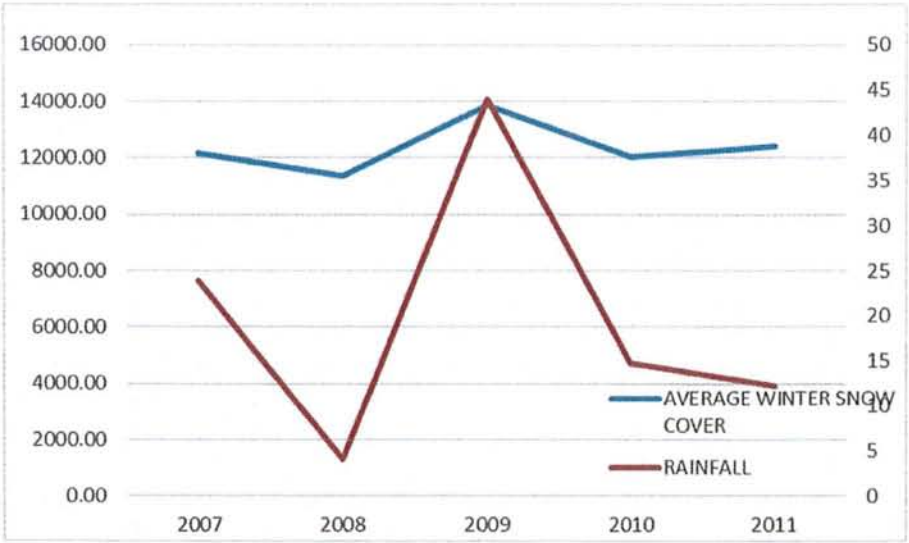

No relation exists between two variables, two main reasons are lack of data duration and very less amount of winter rainfall to correlate.

3.3 Conclusion

The snow cover calculated by using MODIS snow tool and delineating catchment area by ArcGIS software was keenly assessed in detail and it is evidently clear that snow cover area of Hunza river basin is decreasing from period 2003-2011.The maximum and minimum snow cover is also reducing in that region. Many researchers have discussed the effect of ***KARAKORAM ANOMALY***, but my results are not in harmony with this hypothesis.

3.4 Recommendations

Further studies on Hunza river basin should be carried out ranging on larger temporal scale and modeling of various climatic aspects for better management of water resources.

REFRENCES

[1] H. Alexandersson, "A homogeneity test applied to precipitation data," *Journal of climatology,* vol. 6, pp. 661-675, 1986.

[2] R. Allen, L. Pereira, D. Raes, M. Smith, and W. Ab, "Allen_FAO1998, 1–15," ed, 1998.

[3] C. L. Archer and K. Caldeira, "Historical trends in the jet streams," *Geophysical Research Letters,* vol. 35, 2008.

[4] C. Strong and R. E. Davis, "Winter jet stream trends over the Northern Hemisphere," *Quarterly Journal of the Royal Meteorological Society: A journal of the atmospheric sciences, applied meteorology and physical oceanography,* vol. 133, pp. 2109-2115, 2007.

[5] D. J. Seidel, Q. Fu, W. J. Randel, and T. J. Reichler, "Widening of the tropical belt in a changing climate," *Nature geoscience,* vol. 1, pp. 21-24, 2008.

[6] D. Archer, "Contrasting hydrological regimes in the upper Indus Basin," *Journal of Hydrology,* vol. 274, pp. 198-210, 2003.

[7] G. Young and K. Hewitt, "Hydrology research in the upper Indus basin, Karakoram Himalaya, Pakistan," *IAHS Publ,* vol. 190, pp. 139-152, 1990.

[8] D. R. Archer and H. J. Fowler, "Spatial and temporal variations in precipitation in the Upper Indus Basin, global teleconnections and hydrological implications," *Hydrology and Earth System Sciences,* vol. 8, pp. 47-61, 2004.

[9] K. Hewitt, "The Karakoram anomaly? Glacier expansion and the 'elevation effect,'Karakoram Himalaya," *Mountain Research and Development,* vol. 25, pp. 332-340, 2005.

[10] R. L. Armstrong, *The glaciers of the Hindu Kush-Himalayan region: a summary of the science regarding glacier melt/retreat in the Himalayan, Hindu Kush, Karakoram, Pamir, and Tien Shan mountain ranges*: International Centre for Integrated Mountain Development (ICIMOD), 2010.

[11] S. R. Bajracharya and B. R. Shrestha, "The status of glaciers in the Hindu Kush-Himalayan region," International Centre for Integrated Mountain Development (ICIMOD)2011.

[12] M. König, J. G. Winther, and E. Isaksson, "Measuring snow and glacier ice properties from satellite," *Reviews of Geophysics,* vol. 39, pp. 1-27, 2001.

[13] J. Winther, R. Bindschadler, M. Konig, and D. Scherer, "Remote sensing of glaciers and ice sheets," *GEOPHYSICAL MONOGRAPH-AMERICAN GEOPHYSICAL UNION,* vol. 163, p. 39, 2005.

[14] K. Partington, "Discrimination of glacier facies using multi-temporal SAR data," *Journal of Glaciology,* vol. 44, pp. 42-53, 1998.

[15] R. S. Williams, D. K. Hall, and C. S. Benson, "Analysis of glacier facies using satellite techniques," *Journal of Glaciology,* vol. 37, pp. 120-128, 1991.

[16] F. Rau, M. Braun, M. Friedrich, F. Weber, and H. Goßmann, "Radar glacier zones and their boundaries as indicators of glacier mass balance and climatic variability," in *Proceedings of the 2nd EARSeL Workshop-Special Interest Group Land Ice and Snow*, 2000, pp. 317-327.

[17] D. Hall, *Remote sensing of ice and snow*: Springer Science & Business Media, 2012.

[18] D. K. Hall and J. Martinec, "Remote sensing of ice and snow," 1986.

[19] D. K. Hall and J. Martinec, "Applications of remotely derived snow data," in *Remote Sensing of Ice and Snow*, ed: Springer, 1985, pp. 56-81.

[20] A. S. Almas, M. Azam, M. Butt, and S. Amer, "EXPLOITATION OF GEOSPATIAL TECHNIQUES FOR STUDYING THE SNOW AND WATER RUNOFF PARAMETERS."

[21] G. Rasul and Q. Chaudhry, "Global warming and expected snowline shift along Northern Mountains of Pakistan," *Proc. of 1st Asiaclic Sympos. Yokohama, Japan,* 2006.

[22] G. Rasul and D. H. Kazmi, "Climate change and challenges to crop production," in *Proceedings of International Workshop on Plant Conservation & Reversing Desertification. A Way Forward, PMAS Arid Agriculture University, Rawalpindi*, 2011, pp. 81-99.

[23] B. Bookhagen and D. W. Burbank, "Toward a complete Himalayan hydrological budget: Spatiotemporal distribution of snowmelt and rainfall and their impact on river discharge," *Journal of Geophysical Research: Earth Surface,* vol. 115, 2010.

[24] W. W. Immerzeel, P. Droogers, S. De Jong, and M. Bierkens, "Large-scale monitoring of snow cover and runoff simulation in Himalayan river basins using remote sensing," *Remote sensing of Environment,* vol. 113, pp. 40-49, 2009.

[25] T. Bolch, A. Kulkarni, A. Kääb, C. Huggel, F. Paul, J. G. Cogley, *et al.*, "The state and fate of Himalayan glaciers," *Science,* vol. 336, pp. 310-314, 2012.

[26] M. Akhtar, N. Ahmad, and M. J. Booij, "The impact of climate change on the water resources of Hindukush–Karakorum–Himalaya region under different glacier coverage scenarios," *Journal of hydrology,* vol. 355, pp. 148-163, 2008.

[27] G. Ali, S. Hasson, and A. M. Khan, "Climate change: Implications and adaptation of water resources in pakistan," *Global Change Impact Studies Centre (GCISC): Islamabad, Pakistan,* 2009.

[28] S. ul Hasson, L. Gerlitz, U. Schickhoff, T. Scholten, and J. Böhner, "Recent climate change over High Asia," in *Climate change, glacier response, and vegetation dynamics in the Himalaya*, ed: Springer, 2016, pp. 29-48.

[29] M. M. Sheikh, N. Manzoor, M. Adnan, J. Ashraf, and A. Khan, "Climate profile and past climate changes in Pakistan," *Global Change Impact Studies Center (GCISC)-RR-01,* 2009.

[30] M. M. Iqbal, M. A. Goheer, S. A. Noor, K. Salik, H. Sultana, and A. M. Khan, "Climate Change and Rice Production in Pakistan: Calibration, Validation and Application of CERES-Rice Model," *Islamabad: Global Change Impact Studies Centre,* 2009.

[31] F. Bashir and G. Rasul, "Estimation of average snow cover over northern Pakistan," *Pakistan Journal of Meteorology,* vol. 7, pp. 63-69, 2010.

[32] S. B. Cheema, G. Rasul, and D. H. Kazmi, "Evaluation of projected minimum temperatures for northern pakistan," *Pakistan Journal of Meteorology,* vol. 7, 2011.

[33] K. F. Ali and D. H. De Boer, "Spatial patterns and variation of suspended sediment yield in the upper Indus River basin, northern Pakistan," *Journal of Hydrology,* vol. 334, pp. 368-387, 2007.

[34] K. Faran Ali and D. H. De Boer, "Spatial patterns and variation of suspended sediment yield in the upper indus River basin, northern Pakistan," *Journal of hydrology (Amsterdam),* vol. 334, pp. 368-387, 2007.

[35] F. F. Sabins Jr, *Remote sensing--principles and interpretation*: WH Freeman and company, 1987.

[36] R. N. Colwell, "Manual of remote sensing," 1985.

[37] R. Harris, "Satellite remote sensing. An introduction," 1987.

[38] S. L. Ozesmi and M. E. Bauer, "Satellite remote sensing of wetlands," *Wetlands ecology and management,* vol. 10, pp. 381-402, 2002.

[39] C. O. Justice, E. Vermote, J. R. Townshend, R. Defries, D. P. Roy, D. K. Hall, *et al.*, "The Moderate Resolution Imaging Spectroradiometer (MODIS): Land remote sensing for global change research," *IEEE transactions on geoscience and remote sensing,* vol. 36, pp. 1228-1249, 1998.

[40] S. W. Running, C. Justice, V. Salomonson, D. Hall, J. Barker, Y. Kaufmann, *et al.*, "Terrestrial remote sensing science and algorithms planned for EOS/MODIS," *International journal of remote sensing,* vol. 15, pp. 3587-3620, 1994.

[41] A. A. Gitelson, Y. J. Kaufman, and M. N. Merzlyak, "Use of a green channel in remote sensing of global vegetation from EOS-MODIS," *Remote sensing of Environment,* vol. 58, pp. 289-298, 1996.

[42] T. C. Eckmann, D. A. Roberts, and C. J. Still, "Using multiple endmember spectral mixture analysis to retrieve subpixel fire properties from MODIS," *Remote Sensing of Environment,* vol. 112, pp. 3773-3783, 2008.

[43] D. Tanré, Y. Kaufman, M. Herman, and S. Mattoo, "Remote sensing of aerosol properties over oceans using the MODIS/EOS spectral radiances," *Journal of Geophysical Research: Atmospheres,* vol. 102, pp. 16971-16988, 1997.

[44] D. K. Hall and G. A. Riggs, "Accuracy assessment of the MODIS snow products," *Hydrological Processes: An International Journal,* vol. 21, pp. 1534-1547, 2007.

[45] Y. Chen, C. Huang, C. Ticehurst, L. Merrin, and P. Thew, "An evaluation of MODIS daily and 8-day composite products for floodplain and wetland inundation mapping," *Wetlands,* vol. 33, pp. 823-835, 2013.

[46] M. Neteler, "Time series processing of MODIS satellite data for landscape epidemiological applications," *International Journal of Geoinformatics,* vol. 1, pp. 133-138, 2005.

[47] S. Gascoin, O. Hagolle, M. Huc, L. Jarlan, J.-F. Dejoux, C. Szczypta, *et al.*, "A snow cover climatology for the Pyrenees from MODIS snow products," *Hydrology and Earth System Sciences,* vol. 19, pp. 2337-2351, 2015.

[48] V. V. Salomonson, W. Barnes, J. Xiong, S. Kempler, and E. Masuoka, "An overview of the Earth Observing System MODIS instrument and associated data systems performance," in *IEEE International Geoscience and Remote Sensing Symposium*, 2002, pp. 1174-1176.

[49] B. Pradhan, U. Hagemann, M. S. Tehrany, and N. Prechtel, "An easy to use ArcMap based texture analysis program for extraction of flooded areas from TerraSAR-X satellite image," *Computers & geosciences,* vol. 63, pp. 34-43, 2014.

[50] P. J. Wampler, R. R. Rediske, and A. R. Molla, "Using ArcMap, Google Earth, and Global Positioning Systems to select and locate random households in rural Haiti," *International journal of health geographics,* vol. 12, pp. 1-8, 2013.

[51] S. Kumar and M. I. Hassan, "Selection of a landfill site for solid waste management: an application of AHP and spatial analyst tool," *Journal of the Indian Society of Remote Sensing,* vol. 41, pp. 45-56, 2013.

[52] P. HUBERT, "Multifractals as a tool to overcome scale problems in hydrology," *Hydrological sciences journal,* vol. 46, pp. 897-905, 2001.

[53] Y. Shi, G. Xu, Y. Wang, B. A. Engel, H. Peng, W. Zhang, *et al.*, "Modelling hydrology and water quality processes in the Pengxi River basin of the Three Gorges Reservoir using the soil and water assessment tool," *Agricultural water management,* vol. 182, pp. 24-38, 2017.

[54] A.-J. Collados-Lara, D. Pulido-Velazquez, and E. Pardo-Iguzquiza, "A Statistical Tool to Generate Potential Future Climate Scenarios for Hydrology Applications," *Scientific Programming,* vol. 2020, 2020.

[55] R. K. Linsley Jr, M. A. Kohler, and J. L. Paulhus, "Hydrology for engineers," 1975.

[56] S. Beucher, "Watersheds of functions and picture segmentation," in *ICASSP'82. IEEE International Conference on Acoustics, Speech, and Signal Processing*, 1982, pp. 1928-1931.